INVESTIGATION OF MIG WELDING TO CORROSION BEHAVIOR OF HEAT TREATED CARBON STEEL

Shing Shian Ng[1] and Nur Azhani Abd Razak[1*]

[1]Faculty of Mechanical Engineering, University Malaysia Pahang
26600 Pekan, Pahang, Malaysia
*Email: azhani@ump.edu.my
Phone : +609-424-6273 ; Fax : +609-424-6222

ABSTRACT

This paper presents corrosion behaviour of heat treated and welded low carbon steel at different welding voltage and filler materials. Welding process was conducted on butt joint specimens using Metal Inert Gas (MIG) technique at welding voltage range of 19 to 21 V with 1 V interval and filler materials used were ER 308L and ER 70S-6 with 1.2 mm diameter. Heat treatment of full annealing was done to the welded low carbon steel and corrosion behaviour was tested using synthetic seawater environment with 3.5 wt% NaCl. Microstructure changes were observed using Scanning Electron Microscope (SEM). Results showed that, corrosion rate decreased when welding voltage increased as it directly affected welding heat input. The welding heat input was found to have a significant effect to corrosion rate as it changed the ferrite content on the microstructure of the specimens. The decreased in corrosion rate was also found when full annealing process was done to the specimens and the used of ER 70S-6 filler material. From metallographic study, iron oxides and pitting was found on the surface of the exposed area after the corrosion test.

Keywords: Filler material; corrosion behavior; low carbon steel; welding voltage; full annealing.

INTRODUCTION

The modernization of this era expands the demands and applications of carbon steel especially in construction industry and the naval structure builder. A lot of mega steel structure platforms have been designed and constructed to fulfil the exploitation of civilization. Most of these structures are fabricated by technique of welding. However, these weldments usually are more vulnerable to steel corrosion crack than the corresponding base plates, the welded zones represent potential weak links which may limit or impair performance (Saleh et al., 2005). Moreover, the corrosion in seawater is reflected by the fact that most of the common structural metals and alloys are attacked by this liquid or its surrounding environments (Gooch, 1974). Thus, improvements in weldment properties are critical to increase the reliability of high-performance structures utilizing welded carbon materials. Several diagrams have been developed to predict the microstructure in the welding of similar and dissimilar metals (Schaeffler, 1949; Delong, 1974). They also relate various alloy elements in the weld metal that have a remarkable influence on the microstructure (Kotecki and Siewert, 1992; Cleiton et al., 2008). A fundamental study to the properties and microstructure of the welded zone of carbon steel was carried out by means of Metal Inert Gas (MIG) welding with

1

different type of filler materials and parameters. With the electrochemical measurement, the corrosion resistance for each welded area was determined.

MATERIALS AND METHODS

The result collected from the testing process is compared and analysed to investigate the corrosion behaviour of low carbon steel. The chemical composition for the as-received carbon steel is shown in Table 1. Half of the low carbon steel specimens received were heat treated to temperature of 950 ˚C for 2 hours and cooled in the switched off furnace as full annealing process. There are two welding filler materials used for welding process which are ER 308L and ER 70S-6 to butt join the low carbon steel with MIG welding to study the corrosion behaviour of the welded metal. Three different welding voltages were used during the MIG welding. Microstructures of the specimens were observed after welding process. Electrochemical test was carried out with solution of 3.5 wt% NaCl at room temperature and standard atmosphere condition. Scanning electron microscopy images of specimens were observed.

Table 1. Chemical composition for the as received carbon steel.

Material	Chemical Composition, weight %				
	C	Mn	P	S	Si
Specimen	0.10	0.223	<0.01	<0.01	<0.01
AISI 1010	0.08-0.13	0.30-0.60	0.04 (max)	0.05 (max)	0.10 (max)

Table 2. Chemical composition of the welding fillers used.

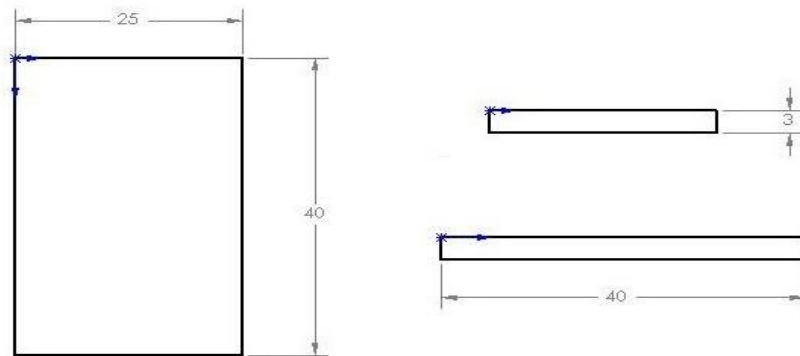| Type of filler	Chemical Composition, weight %					
	C	Mn	P	Si	Cu	Cr
ER 70S	0.06-0.15	1.40-1.85	0.25	0.80-1.15	0.50	0.15
ER 308L	0.03	1.00-2.50	0.03	0.30-0.65	0.75	19.5-22.0

Figure 1. Workpiece dimension in mm.

RESULTS AND DISCUSSIONS

Microstructure Comparison After Heat Treatment Process

From the observation of optical microstructures in Figure 2 for the base metal of (a) non-heat treated and (b) heat treated low carbon steel, there are ferrite (B), pearlite(A) and the grain boundary cementite film (GB) found in the microstructure. By comparison, the amount of pearlite, ferrite and the grain boundary cementite film (GB) were different between non-heat treated and heat treated carbon steel.

The grain size for the heat treated carbon steel is much more differ where it found to be larger than the non-heat treated carbon steel. The specimens were heated to 950˚C for two hour. Here all the ferrite was transform into austenite form. At this heating process, the specimens were homogenized. The carbon steel was then cooled in the realm for gaining the slow cooling rate. This results in a coarse pearlite structure. Full annealed steel is soft and ductile with no internal stress.
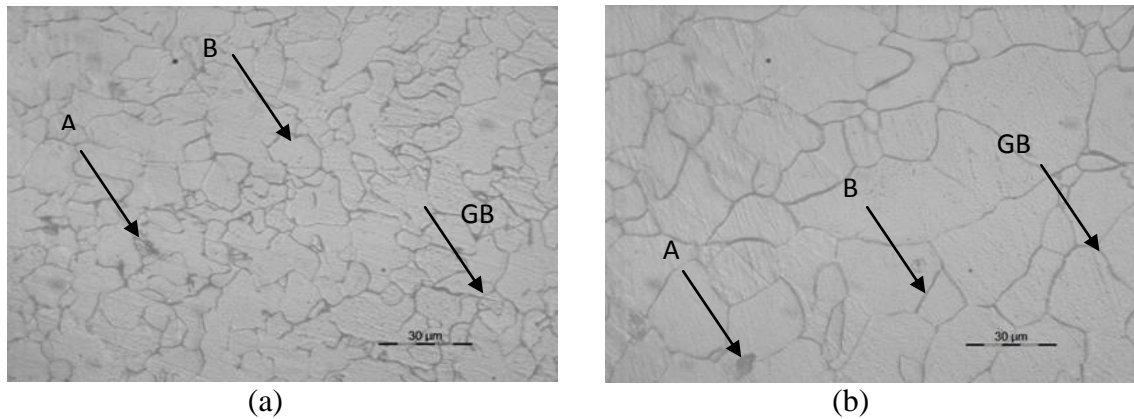

| (a) | (b) |

Figure 2. Microstructures for the base metal: (a) non-heat treated, and (b) heat treated.

Microstructure of Welded Low Carbon Steel

The microstructure of weldment for specimens with welding voltage of 19V and 21V with welding filler ER 70S were compared to study the different in microstructure content. The microstructure on Figure 3 was labelled with PF (polygonal ferrite), FS (aligned side plate ferrite or known as the Widmanstatten ferrite) and AF (acicular ferrite).

The microstructure of weldment for specimen of welding voltage 19V and 21V with ER 70S mild steel filler at non-heat treated condition had different amount of acicular ferrite, polygonal ferrite and the aligned side plate ferrite by observing the images in Figure 4. By comparing both figures, the amount of acicular ferrite in welding voltage of 19V was lower if compared to the weldment which was welded at welding voltage of 21V. The polygonal ferrite, which looked similarly as ferrite inhibit much of the weldment zone in the specimen with welding voltage of 19V. For specimen with welding voltage of 21V, the aligned side plate ferrite/Widmanstatten ferrite and the acicular ferrite inhibit at much of the weldment of the microstructure.

The acicular ferrite found in the microstructure of weldment is actually a microstructure of ferrite which is characterized with the needle shaped crystallites. These grains are actually in thin lenticular shape. This acicular ferrite is benefits to the microstructure as it can increase the toughness of the specimen due to its chaotic

ordering. Acicular ferrite is the microstructure that is advantageous over other microstructures (Udomptol, 2007).

Aligned side plate ferrite or Widmanstatten ferrite in the microstructure of weldment increases as the austenite grain size and the cooling rate of the weldment increased. By decreasing the austenite grain size and increasing the cooling rate, both yield strength and impact toughness will increase (Kumaresh, 2007). The overall refinement of Widmanstatten ferrite attributes the strength and toughness to the microstructure. Polygonal ferrite nucleates at the austenite grain boundaries and in intragranular regions. Polygonal ferrite is transformed at high temperatures and favoured in high heat input processes. Large amount of polygonal ferrite is not considered beneficial to toughness, especially in higher strength steels. It is of lower strength than other transformation products.
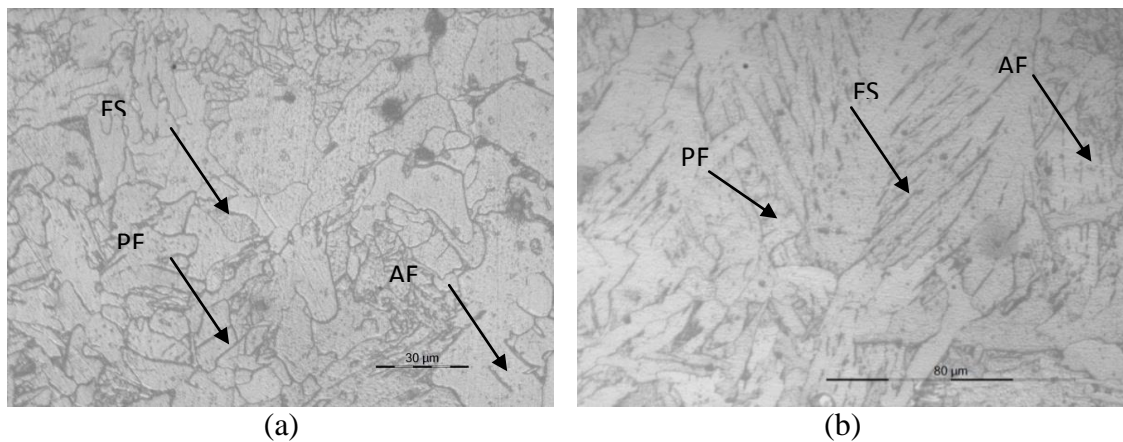

| (a) | (b) |

Figure 3. Microstructure of weldment for non-heat treated specimen welded with ER 70S filler (500x magnification): (a) 19V, and (b) 21V.

Polarization Diagram Analysis

The polarization diagrams for the 12 specimens were generated with the potentiostat of WonaTech WPG100 and shown in Figure 4 and 5. Tafel analysis was performed by extrapolating the linear portions of the logarithm of absolute current density and the corrosion potential plot. The Tafel analysis calculated the corrosion rate of each specimen after importing the value of sample area, density and the equivalent weight in the IVMAN software.
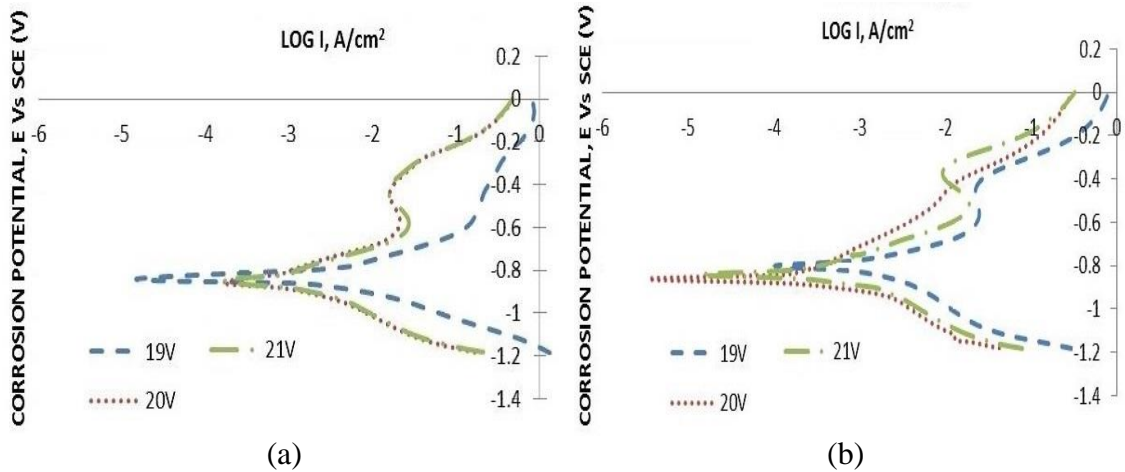
(a)

(b)

Figure 4. Polarization diagram for welded carbon steel with ER 70S filler: (a) non-heated, and (b) heat treated.
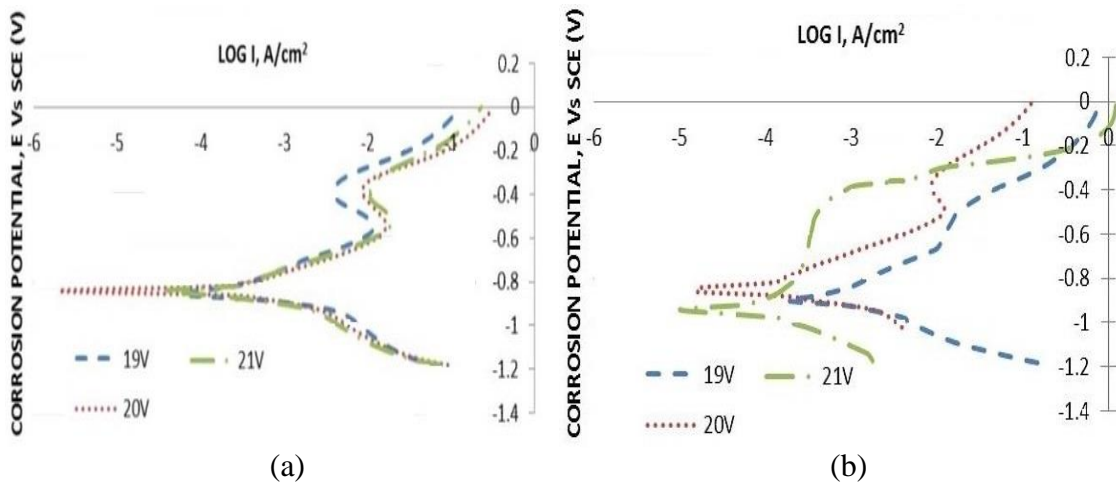

(a)

(b)

Figure 5. Polarization diagram for welded carbon steel with ER 308L filler: (a) non-heated, and (b) heat treated.

Effect of Welding Voltage on the Corrosion Rate

Table 3. Corrosion rate of specimens at different welding parameters.

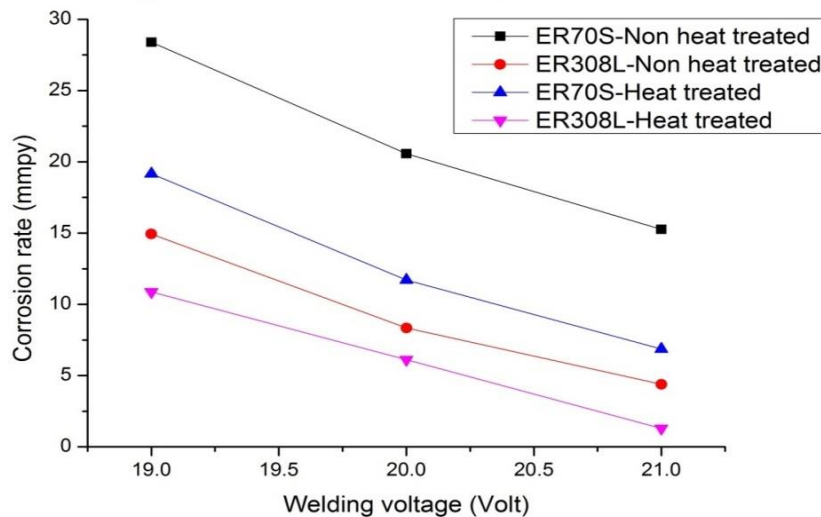| Welding Voltage, V	Corrosion Rate, mmpy			
	Non-heat treated		Heat treated	
	ER 70S (mild steel filler)	ER 308L (stainless steel filler)	ER 70S (mild steel filler)	ER 308L (stainless steel filler)
19	28.4	14.9	19.1	10.8
20	20.5	8.3	11.7	6.1
21	15.2	4.3	6.8	1.2

Figure 6. Graph of corrosion rate versus the welding voltage for welded low carbon steel

From the trend of the graph for both heat treated and non-heat treated carbon steel in Figure 6, the corrosion rate of the specimen was decreased as the welding voltage increases. The non-heated carbon steel has higher corrosion when compared to the heat treated carbon steel. The heat treated carbon steels have the lower corrosion rate because the materials were heat treated at full annealing process. The heat treated carbon steel has higher corrosion resistance by comparing to the non-heat treated materials.

The specimens welded with the ER 308L stainless steel filler has lower corrosion compare to the welding filler of ER 70S. The chemical composition of the ER 70S and ER 308L filler were showed in the Table 2. ER 308L filler has lower carbon content and higher chromium content compared to the ER 70S filler. The high chromium contains in the ER 308L filler make it resist rust than other type of steel. The chromium combines with oxygen in the atmosphere to form a thin invisible layer – passive film. If the materials are cut or scratched and the passive film is disrupted, more oxide will quickly form and recover the exposed surface, protecting it from oxidative corrosion.

As the welding voltage increases, the welding heat input will increase and increase the welding temperature. The welding temperature will affect the microstructure changes on the weldment. This microstructure changes were shown in Figure 4. The different of welding voltage will have the different microstructure on the weldment. By comparing images in Figure 4, the weldment with welding voltage of 20V had more polygonal ferrite which was considered not beneficial to the toughness of the specimen. The weldment with welding voltage of 21V had large amount of acicular ferrite and aligned side plate ferrite which contribute to the strength and toughness on the welded low carbon steel. The weldment for specimen of welding voltage 21V has the better mechanical properties due to the ferrites content in the microstructure. In other words, the higher welding heat input will have the lower corrosion rate for the welded low carbon steel.

Scanning Electron Microscopy Result

The SEM in Figure 7 showed the images of specimen without cleaning process. The corrosion exist due to the exposed of surface area after electrochemical testing. The shapes of coral alike were found in the SEM image. The corrosion products formed on the surface of the specimen were iron oxides or in general term named rust (Iversen and Leffler, 2010). These iron oxides consist of iron (III) oxides and iron (III) oxide-hydroxide.

The SEM of specimen after cleaning process was showed in Figure 8. After cleaning process, there were pits found on the surface of specimen (Garner, 1979; Noor, et al., 2008). Pitting is a form of extremely localized attack that results in holes in the metal. These holes may be small or large in diameter but in most cases they are relatively small. It is difficult to detect pits because of their small size and pits are often covered with corrosion products.
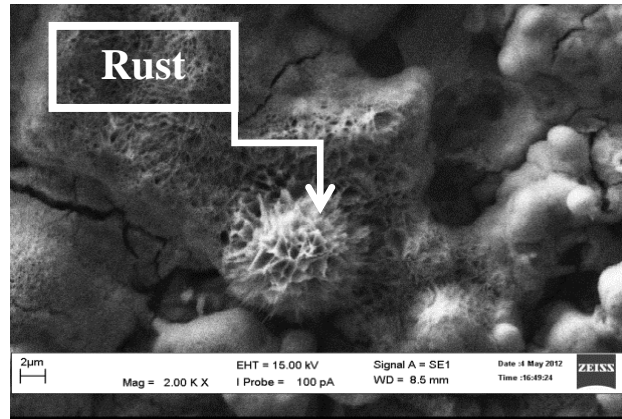

Figure 7. Corrosion product formed after corrosion test (2000x magnification).
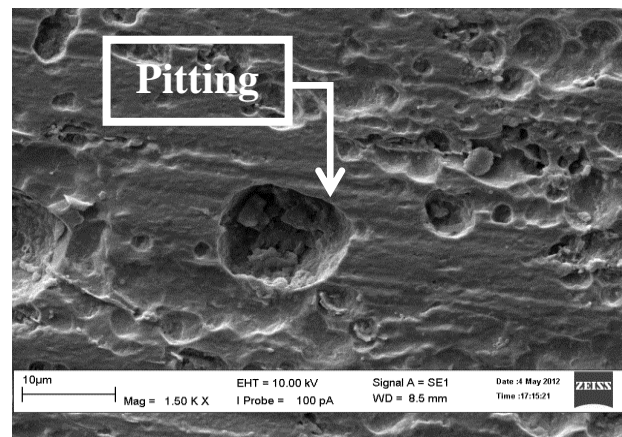

Figure 8. Corrosion defect after corrosion test (1500x magnification).

CONCLUSION

In conclusion, the corrosion behaviour of MIG welded heat treated carbon steel was investigated. The welding heat input has the significant to the corrosion rate of the carbon steel where high welding heat input will produce a welded carbon steel with low corrosion rate. This welding temperature will affect the microstructures changes on the weldment and vary the properties of the welded carbon steel. For the overall results comparison, welding heat input has the most significant to the corrosion rate of the welded carbon steel with take up to 42.68% affection. The types of welding fillers used conclude 34.97% to the corrosion rate while the carbon steels' treatment inhibit total of 22.35% to the corrosion rate of the welded carbon steel.

ACKNOWLEDGEMENTS

REFERENCES

Delong, W.T. 1974. Ferrite in austenitic stainless steel weld metal. Weld. 53: 273.

Garner, A. 1979 The effect of autogeneous welding on chloride pitting corrosion in austenitic stainless steels, Corrosion. 35: 108-114.

Gooch, T.G. 1974. Welding. 53 (7): 287.

Iversen, A. and Leffler, B. 2010. Aqueous corrosion of stainless steel, Ferrous Metal and Alloys. 1806-1877.

Kotecki, D.J. and Siewert, T.A. 1992. Constitution diagram for stainless steel weld metals: a modification of the WRC-1988 diagram. Weld. 71: 171.

Kumaresh, S.P. 2007. Influence of heat input on high temperature weldment corrosion in submerged arc welded power plant carbon steel, Materials and Design. 29: 1036-1042.

Noor, E.A., and Al-Moubaraki, A.H. 2008. Corrosion behaviour of mild steel in hydrochloric acid solutions, International Journal Electrochemical Science. 3: 806-818.

Saleh, A., Al-Fozan, and Anees Malik, U. 2005. Effect of seawater level on corrosion behavior of different alloys. Desalination. 3 (228): 61-67.

Schaeffler, A.L. 1949. Constitution diagram for stainless steel weld metal. Stainless Steel. 56: 680.

Schino, A.D., Mecozzi, M.G., Barteri, M., and Kenny, J.M. 2000. Solidification mode and residual ferrite in low-Ni austenitic stainless steels. Materials Science. 35: 375.

Silva, C.C., Miranda, H.C., Sant'Ana, H., and Farias, J.P. 2008. Microstructure,hardness and petroleum corrosion evaluation of 316L/AWS E309 MoL-16 weld metal, Material Characterization. 60: 346-352.

Udomphol, T. 2007. Solidification and phase transformations in welding.